PALEOCEANOGRAPHY

Nitrogen isotope evidence for expanded ocean suboxia in the early Cenozoic

Emma R. Kast[1]*, Daniel A. Stolper[2,3], Alexandra Auderset[4,5], John A. Higgins[1], Haojia Ren[6], Xingchen T. Wang[7], Alfredo Martínez-García[4], Gerald H. Haug[4,5], Daniel M. Sigman[1]

The million-year variability of the marine nitrogen cycle is poorly understood. Before 57 million years (Ma) ago, the $^{15}N/^{14}N$ ratio ($\delta^{15}N$) of foraminifera shell-bound organic matter from three sediment cores was high, indicating expanded water column suboxia and denitrification. Between 57 and 50 Ma ago, $\delta^{15}N$ declined by 13 to 16 per mil in the North Pacific and by 3 to 8 per mil in the Atlantic. The decline preceded global cooling and appears to have coincided with the early stages of the Asia-India collision. Warm, salty intermediate-depth water forming along the Tethys Sea margins may have caused the expanded suboxia, ending with the collision. From 50 to 35 Ma ago, $\delta^{15}N$ was lower than modern values, suggesting widespread sedimentary denitrification on broad continental shelves. $\delta^{15}N$ rose at 35 Ma ago, as ice sheets grew, sea level fell, and continental shelves narrowed.

Biologically available nitrogen (or "fixed N") is needed by all organisms and commonly limits biological productivity. Accordingly, the cycling of fixed N is tightly linked to that of carbon and oxygen (O_2) in the ocean. Dinitrogen (N_2) fixation by cyanobacteria in surface waters is the ocean's main source of fixed N (*1*). The dominant sink is denitrification, the biological reduction of nitrate (NO_3^-) to N_2 during the oxidation of organic matter at low O_2 availability (*1*). Denitrification occurs in (i) marine sediments, where rates are largely determined by organic matter flux, and (ii) O_2-depleted (suboxic or anoxic) zones of the thermocline and intermediate-depth water column, which occur today in the eastern tropical Pacific and the Arabian Sea (*1*).

Given that water column denitrification requires suboxia, the marine N cycle may have responded to changes in ocean O_2 content in the geological past (*2*, *3*). Over the Cenozoic era [66 million years (Ma) ago to the present], deep ocean temperatures declined by 8° to 10°C (*4*), which would have increased the solubility of O_2 in seawater by roughly 20% (*5*). Here, we report records of the $\delta^{15}N$ {defined as $[(^{15}N/^{14}N_{sample})/(^{15}N/^{14}N_{air}) - 1] \times 1000$}, of organic matter bound within fossil planktonic foraminifera shells (foraminifera-bound $\delta^{15}N$, FB-$\delta^{15}N$) (*6*) from 70 to 30 Ma ago to examine the ocean N cycle across this period of global cooling.

Ocean nitrate records the combined N isotopic signals of the inputs (mainly N_2 fixation) and outputs (mainly denitrification) of fixed N to and from the ocean (*7*). N_2 fixation produces oceanic fixed N with a $\delta^{15}N$ of approximately −1 per mil (‰) (*8*, *9*). Sedimentary denitrification typically removes nitrate from the ocean with minimal isotopic discrimination owing to complete nitrate consumption in the sediment porewaters (*10*). In contrast, water column denitrification expresses a strong preference for ^{14}N-bearing nitrate (with an isotopic discrimination of ~15 to 25‰), causing the residual nitrate to be enriched in ^{15}N in the shallow subsurface water column within and near the suboxic zones (*11*). Water column denitrification is largely responsible for the elevation of global mean ocean nitrate $\delta^{15}N$ relative to newly fixed N (5 and −1‰, respectively) (*12*).

The production of N-containing biomass in the surface ocean is fueled by nitrate supplied from the shallow subsurface (~100 to 300 m depth), and this nitrate reflects both the $\delta^{15}N$ of mean ocean nitrate and any regional isotopic imprint of N_2 fixation and/or water column denitrification. In regions of complete nitrate consumption, both bulk sedimentary N and foraminifera-bound N have been shown to reflect variations in the $\delta^{15}N$ of the shallow subsurface nitrate (*13*–*15*). Most existing N isotope records are of bulk sediment (*2*, *3*, *16*). In contrast to bulk sedimentary organic matter, foraminifera-bound organic matter is isolated within, and thus protected by, the mineral matrix of the foraminifera shell wall, making it less vulnerable to isotopic alteration during burial or to contamination by exogenous N sources (*14*, *17*, *18*). Measurements of bulk sediment N content and $\delta^{15}N$ confirm the benefit of FB-$\delta^{15}N$ for our study of millions-of-years-old sediment records (fig. S1). Most of the data presented here are on sieved size fractions of foraminifera shells of mixed taxa (*6*). By analyzing picked foraminiferal genera for FB-$\delta^{15}N$ at select depths, we verified that the mixed taxa FB-$\delta^{15}N$ is not controlled by changes in the abundance of taxa with different FB-$\delta^{15}N$ (figs. S2 and S3).

We report FB-$\delta^{15}N$ records from three Ocean Drilling Program (ODP) sites: one each in the North Pacific, North Atlantic, and South Atlantic (Fig. 1 and table S1) (*19*–*21*). The paleo-locations of the sites suggest that all were characterized by

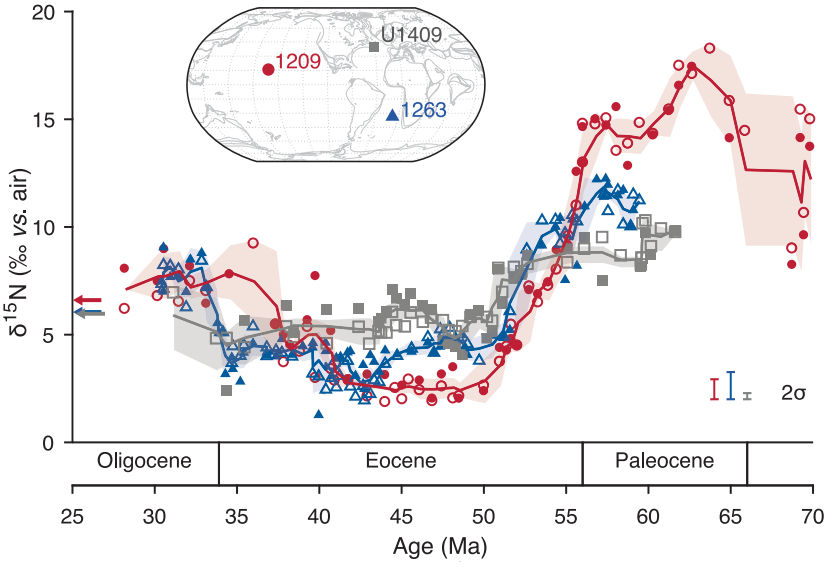

Fig. 1. Foraminifera-bound $\delta^{15}N$ from 70 to 30 Ma ago. Size fractions of >250 μm (closed symbols) and 125 to 250 μm (open symbols) from ODP Site 1209 (red circles), ODP Site 1263 (blue triangles), and IODP Site U1409 (gray squares). Correspondingly colored bold lines represent the three-point moving average across both size fractions, with shaded uncertainty intervals indicating their 1σ. Representative error bars in the lower right show the average 2σ for all the replicates analyzed for each site (*6*). Arrows on the left indicate core-top FB-$\delta^{15}N$ values from South Atlantic Site 516 (blue) and Site U1409 (gray), which overlap, and Site 1209 (red). Inset map shows a global plate reconstruction at 55 Ma ago (*46*), with markers indicating the estimated paleo-locations for the ODP and IODP sites used in this study. Geologic epochs are based on GTS2012 (*47*).

complete nitrate consumption at the surface (*6*). As such, FB-$\delta^{15}N$ should reflect the $\delta^{15}N$ of shallow subsurface nitrate (*14*, *15*). At all sites, FB-$\delta^{15}N$ decreases from 57 to 50 Ma ago in the Paleocene to early Eocene (Fig. 1). The largest FB-$\delta^{15}N$ decline occurs at Site 1209 in the North Pacific: From 57 to 50 Ma ago, FB-$\delta^{15}N$ decreases from >15 to 2‰. At Site 1263 in the South Atlantic, the change occurs with similar timing but is of a lower magnitude, from 11 to <5‰. The International Ocean Discovery Program (IODP) Site U1409 in the Northwest Atlantic shows a still smaller change, from 9 to 5‰. After a period of relatively stable and low FB-$\delta^{15}N$ through the middle Eocene, FB-$\delta^{15}N$ at Sites 1209 and 1263 increases in the late Eocene, reaching 7 to 8‰ in the Oligocene; the Eocene-to-Oligocene change at Site U1409 is currently not well resolved. Although these changes were not observed in previous bulk sediment studies (fig. S4) (*2*), they are evident in our limited set of bulk sediment $\delta^{15}N$ measurements, albeit with lower amplitude and less clarity than in FB-$\delta^{15}N$ (fig. S1).

As this is the first application of FB-$\delta^{15}N$ to the million-year time scale, the potential impact of diagenesis was considered with multiple lines of evidence. Together, they indicate that the FB-$\delta^{15}N$ changes are best interpreted as primary (*22*). A major role for diagenesis in the FB-$\delta^{15}N$ records is inconsistent with (i) the coincidence of FB-$\delta^{15}N$ changes across distant records, regardless of depth in the sediment; (ii) a positive (not negative) correlation between FB-$\delta^{15}N$ and FB-N content; and (iii) a lack of correlation of FB-$\delta^{15}N$ and FB-N content with other sedimentary properties [among other observations (*22*)]. Prior studies indicate that FB-N content changes associated with early diagenesis of foraminiferal shells do not affect FB-$\delta^{15}N$ (*15*). These findings are consistent with the chemically labile, amino acid–dominated composition of FB-N (*23*, *24*): The exposure of FB-N due to calcite diagenesis should lead to complete loss of the exposed N rather than the survival of an isotopically altered residuum. We proceed with the interpretation that the FB-$\delta^{15}N$ records indicate past changes in the $\delta^{15}N$ of shallow subsurface nitrate.

Paleocene FB-$\delta^{15}N$ is ~5 to 10‰ higher than core-top FB-$\delta^{15}N$ in the studied regions (Fig. 1), suggesting a higher Paleocene global mean ocean nitrate $\delta^{15}N$. Mean ocean nitrate $\delta^{15}N$ dominantly reflects the relative rate of water column versus sedimentary denitrification (*7*, *12*, *25*), with a high mean ocean nitrate $\delta^{15}N$ indicating either a high global-ocean rate of water column denitrification or a low rate of sedimentary denitrification.

The FB-$\delta^{15}N$ differences among the sites support the first alternative: enhanced water column denitrification during the Paleocene. Water column denitrification causes strong spatial gradients in shallow subsurface nitrate $\delta^{15}N$ (*26*) and thus can explain the FB-$\delta^{15}N$ elevation at Site 1209 relative to Sites 1263 and U1409 during the Paleocene. Moreover, among these three sites, the late Paleocene to early Eocene FB-$\delta^{15}N$ decline was greatest at Site 1209, as would be expected if the $\delta^{15}N$ of the nitrate supply at Site 1209 was lowered by declines both in global mean ocean nitrate $\delta^{15}N$ and in regional nitrate $\delta^{15}N$ elevation associated with nearby water column denitrification (*22*). These findings imply that the Pacific hosted water column denitrification during the Paleocene, as it does today, but at greater rates.

Elevated water column denitrification points to more extensive suboxia in the Paleocene ocean. This is consistent with planktonic foraminiferal I/Ca data from just before the Paleocene-Eocene thermal maximum (*27*). Two mechanisms could increase suboxia: (i) higher export production or (ii) lower starting (preformed) dissolved O_2 concentrations. We are unaware of any evidence for, or reason to expect, higher export production in the Paleocene (*28*). The globally warmer conditions of the early Cenozoic would have lowered preformed O_2 by reducing O_2 solubility in surface waters. However, if global climate were the sole driver, FB-$\delta^{15}N$ and global temperature would be positively correlated, with cooling leading to higher preformed O_2, less expansive suboxia, less water column denitrification, and thus lower FB-$\delta^{15}N$. In contrast, most of the $\delta^{15}N$ decline from high Paleocene values precedes Eocene cooling as recorded in benthic foraminifera $\delta^{18}O$ (Fig. 2) (*29*). Instead, the $\delta^{15}N$ decline coincides with the approach to the early Eocene climate optimum at 50 Ma ago. Global warmth may have contributed to the enhanced Paleocene suboxia and denitrification; however, the mismatch in timing indicates that it alone was insufficient.

[1]Department of Geosciences, Princeton University, Princeton, NJ 08540, USA. [2]Department of Earth and Planetary Science, University of California, Berkeley, CA 94720, USA. [3]Earth and Environmental Sciences Area, Lawrence Berkeley National Laboratory, Berkeley, CA 94720, USA. [4]Department of Climate Geochemistry, Max Planck Institute for Chemistry, 55128 Mainz, Germany. [5]Department of Earth Sciences, ETH Zürich, CH-8092 Zürich, Switzerland. [6]Research Center for Future Earth, National Taiwan University, Taipei 106, Taiwan. [7]Division of Geological and Planetary Sciences, California Institute of Technology, Pasadena, CA 91125, USA.
***Corresponding author. Email: ekast@princeton.edu**

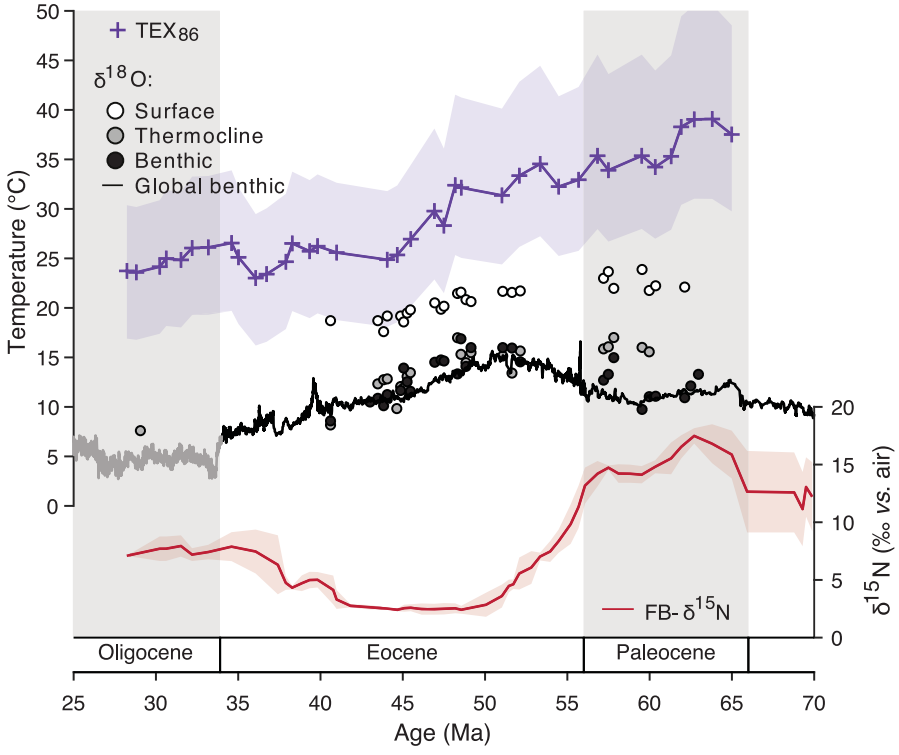

Fig. 2. Comparison of FB-$\delta^{15}N$ and temperature proxy changes at Site 1209 in the North Pacific. TEX_{86} values (purple crosses) are converted to sea surface temperatures using the calibration of (*48*). TEX_{86} measurements are connected by a bold line; shaded purple region indicates the 90% confidence interval of the temperature calibration. Temperatures were calculated from the calcite $\delta^{18}O$ of surface- and thermocline-dwelling planktonic foraminifera and benthic foraminifera from Site 1209 (*41*) and from a benthic foraminifera $\delta^{18}O$ global compilation (*29*), using the equation of (*49*) as in (*4*, *41*); the gray interval for the benthic foraminiferal line indicates when ice volume change likely compromises this calculation. The FB-$\delta^{15}N$ moving average is as in Fig. 1. Gray background indicates Paleocene and Oligocene epochs.

During the Cenozoic, India and Africa converged on Eurasia, closing the Tethys Sea, with the first manifestations of the collision at 59 Ma ago, coincident with the start of the $\delta^{15}N$ decline (*30*, *31*). The Tethys was surrounded by extensive shallow seas, located at subtropical latitudes where seawater evaporation exceeds precipitation (*30*). We propose that formation of warm, salty subsurface waters in these shallow seas introduced water with low preformed O_2 into the thermocline and/or intermediate-depth waters of the global ocean, expanding suboxia and thus water column denitrification (Fig. 3). This hypothesis is inspired by previous suggestions of warm and salty deep water formation in warmer climates (*32*, *33*) but involves thermocline and intermediate depths only and thus does not contradict observational and modeling evidence for high-latitude deep water formation during this time (*29*, *34*–*36*). Modern analogs for the proposed Tethys water are the Mediterranean and Red Sea outflow waters, although these are not currently formed and exported at rates adequate to strongly affect the global ocean's thermocline or intermediate-depth O_2 concentration.

We propose that changes accompanying the closure of the Tethys (*30*) effectively ended the ventilation of the ocean's thermocline and intermediate depths by warm, salty, low-preformed-O_2 Tethys water. This could have been due to a loss of shelf environments needed for forming Tethys water or the development of new bathymetric features that impeded its export to the open ocean. In either case, this lost low-latitude source of ventilation would have been replaced by colder and thus more O_2-rich high-latitude source regions, which dominate today (e.g., the sub-Antarctic zone of the Southern Ocean). Higher preformed O_2 in thermocline and intermediate-depth waters would have contracted the suboxic zones (Fig. 3), reducing water column denitrification and lowering nitrate $\delta^{15}N$. The $\delta^{15}N$ decrease is nearly coincident with a conspicuous rise in the $\delta^{34}S$ of barite and foraminifera carbonate-associated sulfate (fig. S5) (*37*–*39*). The $\delta^{34}S$ rise has also been interpreted as the consequence of the India-Asia collision and a resulting decline in the extent of shallow continental shelves (*39*).

Our hypothesis makes the prediction that the temperature difference between the thermocline and deep ocean should have declined from the Paleocene to early Eocene, because of a change in the source of thermocline water from the warm, salty Tethys to the colder high-latitude surface ocean. As a step toward constraining thermocline and intermediate-depth water temperature, we used the TEX_{86} proxy to reconstruct sea surface temperature (SST) at Site 1209 (*40*). Benthic foraminifera $\delta^{18}O$ records a warming in deep waters from 57 to 50 Ma ago (*29*, *41*), whereas the TEX_{86} data from Site 1209 indicate that SST decreased continuously from ~62 to 30 Ma ago (Fig. 2). The resulting convergence of deep and surface temperature from 57 to 50 Ma ago is consistent with a change in the source of Pacific thermocline and intermediate-depth waters from a warmer, lower-preformed-O_2 source to a colder, higher-preformed-O_2 source over the time that FB-$\delta^{15}N$ declined (Fig. 2 and fig. S6). Measurements of planktonic foraminifera $\delta^{18}O$ from Site 1209 (*41*) corroborate this interpretation (Fig. 2), with additional evidence from different taxa of planktonic foraminifera that the convergence toward deep ocean temperature was greater at thermocline depths than at the surface (fig. S6).

During the middle Eocene, FB-$\delta^{15}N$ at all sites was lower than core-top FB-$\delta^{15}N$ (Fig. 1), suggesting that Eocene mean ocean nitrate $\delta^{15}N$ was lower than modern. One possible explanation is that sedimentary denitrification fluxes were higher than modern due to a greater area of submerged continental shelves before the growth of the Antarctic ice sheet at the Eocene-Oligocene transition (Fig. 3) (*30*). Because these shelves would have also been present before 50 Ma ago, the high ocean nitrate $\delta^{15}N$ in the Paleocene was achieved despite such higher rates of sedimentary denitrification. This implies an even greater global rate of water column denitrification during the Paleocene.

Around the Eocene-Oligocene transition (33.9 Ma ago), FB-$\delta^{15}N$ increases by 4 to 5‰ in both the Atlantic and Pacific (Sites 1209 and 1263) (Fig. 1). This suggests an increase in mean ocean nitrate $\delta^{15}N$ without a strengthening of the regional nitrate $\delta^{15}N$ gradients, pointing to a change in sedimentary rather than water column denitrification. The Eocene-Oligocene transition is marked by the expansion of Antarctic ice sheets, lower global sea level, and a reduction in the area of submerged continental shelves (*30*, *42*). We propose that the Eocene-Oligocene increase in FB-$\delta^{15}N$ occurred because of a decline in shelf-hosted sedimentary denitrification due to this ice sheet growth (Fig. 3).

The FB-$\delta^{15}N$ records presented above suggest large changes in the fluxes of water column and sedimentary denitrification. Here, we use a simple steady-state isotope mass balance calculation to provide first-order estimates of the potential scale of the proposed changes in the inputs and outputs of marine fixed N (Fig. 3) (*6*). We derive the mean ocean nitrate $\delta^{15}N$ from the average of the Atlantic records and assume that Oligocene N fluxes were similar to modern (*6*, *43*). This calculation suggests that the global rate of sedimentary denitrification was almost two times higher in the Eocene and Paleocene than in the Oligocene (250 versus 130 Tg N/year) and that the rate of water column denitrification was 3.5 times higher in the Paleocene than in the Oligocene and Eocene (210 versus 60 Tg N/year) (Fig. 3 and table S2). We estimate that the net global marine denitrification rate during the Paleocene was more than twice the modern

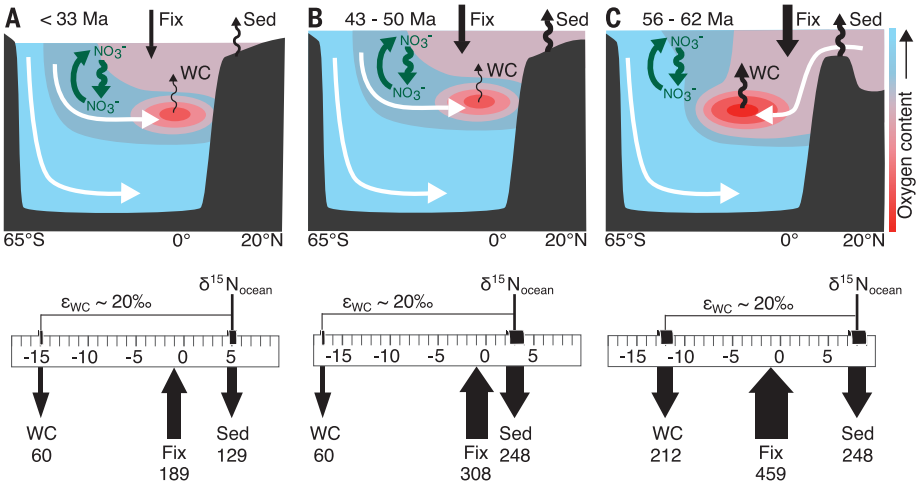

Fig. 3. Proposed mechanisms and N flux calculations for the major FB-$\delta^{15}N$ changes. Panels represent the oxygen concentrations and N cycle fluxes of the global ocean (**A**) after the Eocene-Oligocene transition, (**B**) during the middle Eocene, and (**C**) before the early Eocene FB-$\delta^{15}N$ decline. (Top panels) White arrows show proposed ventilation of ocean interior, with oxygen content indicated by color; black arrows show the input of fixed N to the ocean by N_2 fixation (straight) and the losses of fixed N by water column and sedimentary denitrification (wavy), with arrow width proportional to calculated N flux; gray-green arrows represent the internal cycling of fixed N. (Bottom panels) Results of the one-box, steady-state isotope mass balance calculations, with arrow positions reflecting the $\delta^{15}N$ of the N fluxes and arrow widths reflecting the flux magnitudes ("Fix" for N_2 fixation, "WC" for water column denitrification, and "Sed" for sedimentary denitrification). Flux estimates are given in teragrams of nitrogen per year (Tg N/year, where 1 Tg is 10^{12} g). It is assumed that the N input from N_2 fixation has a $\delta^{15}N$ of −1‰ and that its rate equals the summed rates of N loss by water column and sedimentary denitrification. It is assumed that water column denitrification occurs with an isotope effect, ε_{WC}, of 20‰ and that sedimentary denitrification expresses no isotope effect. The modern water column denitrification flux is used for (A) (*43*); all other fluxes are calculated from mean ocean nitrate $\delta^{15}N$ based on the two Atlantic FB-$\delta^{15}N$ records [see text and (*6*)].

rate (460 versus 190 Tg N/year). Increased denitrification requires a compensatory increase in N_2 fixation during the Paleocene to prevent the ocean from losing its fixed N in a matter of millennia. It is not clear whether this balance was struck at a N reservoir size similar to that of the modern ocean. Today, N_2 fixation is typically less important than subsurface nitrate in the annual supply of fixed N to surface waters (*9*); in the Paleocene, the higher rate of N_2 fixation would have made these two supply terms more comparable (Fig. 3).

Our study of early Cenozoic FB-$\delta^{15}N$ indicates that tectonics, through its effect on ocean circulation, can substantially alter global biogeochemistry. In past extinction events (*44*) and under future global warming (*45*), declining ocean oxygen has been implicated as a driver of biotic and geochemical change. Ocean circulation influences the oxygen content of thermocline and intermediate-depth water, in part by dictating the water's source region and thus its temperature and starting oxygen concentration. Over the early Cenozoic, it appears that ocean circulation was more important than global average temperature in modulating oxygen depletion and denitrification in the ocean interior.

REFERENCES AND NOTES

1. N. Gruber, in *Nitrogen in the Marine Environment*, D. G. Capone, D. A. Bronk, M. R. Mulholland, E. J. Carpenter, Eds. (Elsevier, ed. 2, 2008), pp. 1–50.
2. T. J. Algeo, P. A. Meyers, R. S. Robinson, H. Rowe, G. Q. Jiang, *Biogeosciences* **11**, 1273–1295 (2014).
3. Z.Liu, M. A. Altabet, T. D. Herbert, *Geochem. Geophys. Geosyst.* **9**, Q11006 (2008).
4. J. Zachos, M. Pagani, L. Sloan, E. Thomas, K. Billups, *Science* **292**, 686–693 (2001).
5. H. E. Garcia, L. I. Gordon, *Limnol. Oceanogr.* **37**, 1307–1312 (1992).
6. See materials and methods in the supplement.
7. D. M. Sigman, F. Fripiat, in *Marine Biogeochemistry*, vol. 1 of *Encyclopedia of Ocean Sciences*, J. K. Cochran, H. Bokuniewicz, P. Yager, Eds. (Academic Press, ed. 3, 2019), pp. 263–278.
8. E. Wada, A. Hattori, *Geochim. Cosmochim. Acta* **40**, 249–251 (1976).
9. A. N. Knapp, P. J. Difiore, C. Deutsch, D. M. Sigman, F. Lipschultz, *Global Biogeochem. Cycles* **22**, GB3014 (2008).
10. J. A. Brandes, A. H. Devol, *Geochim. Cosmochim. Acta* **61**, 1793–1801 (1997).
11. J. D. Cline, I. R. Kaplan, *Mar. Chem.* **3**, 271–299 (1975).
12. C. Deutsch, D. M. Sigman, R. C. Thunell, A. N. Meckler, G. H. Haug, *Global Biogeochem. Cycles* **18**, GB4012 (2004).
13. M. A. Altabet, in *Marine Organic Matter: Biomarkers, Isotopes and DNA*, J. K. Volkman, Ed., vol. 2N of *The Handbook of Environmental Chemistry* (Springer, 2006), pp. 251–293.
14. H. Ren, D. M. Sigman, R. C. Thunell, M. G. Prokopenko, *Limnol. Oceanogr.* **57**, 1011–1024 (2012).
15. S. M. Smart *et al.*, *Geochim. Cosmochim. Acta* **235**, 463–482 (2018).
16. R. S. Robinson *et al.*, *Paleoceanography* **27**, PA4203 (2012).
17. H. Ren *et al.*, *Science* **323**, 244–248 (2009).
18. M. A. Altabet, W. B. Curry, *Global Biogeochem. Cycles* **3**, 107–119 (1989).
19. Shipboard Scientific Party, in *Proceedings of the Ocean Drilling Program, Initial Reports*, vol. 198 (ODP, 2002), chap. 5.
20. Shipboard Scientific Party, in *Proceedings of the Ocean Drilling Program, Initial Reports*, vol. 208 (ODP, 2004), chap. 4.
21. R. D. Norris *et al.*, in *Proceedings of the Integrated Ocean Drilling Program*, vol. 342 (IODP, 2014).
22. See supplementary text in the supplement.
23. A. E. Ingalls, C. Lee, S. G. Wakeham, J. I. Hedges, *Deep-Sea Res. Part II* **50**, 713–738 (2003).
24. K. King Jr., P. E. Hare, *Science* **175**, 1461–1463 (1972).
25. J. A. Brandes, A. H. Devol, *Global Biogeochem. Cycles* **16**, 1120 (2002).
26. D. M. Sigman *et al.*, *Deep Sea Res. Part I* **56**, 1419–1439 (2009).
27. X. Zhou, E. Thomas, R. E. M. Rickaby, A. M. E. Winguth, Z. Lu, *Paleoceanography* **29**, 964–975 (2014).
28. M. Lyle *et al.*, *Rev. Geophys.* **46**, RG2002 (2008).
29. B. S. Cramer, J. R. Toggweiler, J. D. Wright, M. E. Katz, K. G. Miller, *Paleoceanography* **24**, PA4216 (2009).
30. W. Cao *et al.*, *Biogeosciences* **14**, 5425–5439 (2017).
31. X. Hu *et al.*, *Earth Sci. Rev.* **160**, 264–299 (2016).
32. T. C. Chamberlin, *J. Geol.* **14**, 363–373 (1906).
33. G. W. Brass, J. R. Southam, W. H. Peterson, *Nature* **296**, 620–623 (1982).
34. D. J. Thomas, R. L. Korty, M. Huber, J. A. Schubert, B. Haines, *Paleoceanography* **29**, 454–469 (2014).
35. T. D. Herbert, J. L. Sarmiento, *Geology* **19**, 702–705 (1991).
36. K. L. Bice, E. J. Barron, W. H. Peterson, *Geology* **25**, 951–954 (1997).
37. A. Paytan, M. Kastner, D. Campbell, M. H. Thiemens, *Science* **282**, 1459–1462 (1998).
38. A. C. Kurtz, L. R. Kump, M. A. Arthur, J. C. Zachos, A. Paytan, *Paleoceanography* **18**, 1090 (2003).
39. V. C. F. Rennie *et al.*, *Nat. Geosci.* **11**, 761–765 (2018).
40. S. Schouten, E. C. Hopmans, E. Schefuß, J. S. Sinninghe-Damsté, *Earth Planet. Sci. Lett.* **204**, 265–274 (2002).
41. A. Dutton, K. C. Lohmann, R. M. Leckie, *Paleoceanography* **20**, PA3004 (2005).
42. A. J. P. Houben, C. A. van Mourik, A. Montanari, R. Coccioni, H. Brinkhuis, *Palaeogeogr. Palaeoecol.* **335–336**, 75–83 (2012).
43. T. DeVries, C. Deutsch, P. A. Rafter, F. Primeau, *Biogeosciences* **10**, 2481–2496 (2013).
44. P. B. Wignall, R. J. Twitchett, *Science* **272**, 1155–1158 (1996).
45. R. J. Matear, A. C. Hirst, *Global Biogeochem. Cycles* **17**, 1125 (2003).
46. M. Seton *et al.*, *Earth Sci. Rev.* **113**, 212–270 (2012).
47. F. M. Gradstein, J. G. Ogg, M. Schmitz, G. Ogg, Eds., *The Geologic Time Scale 2012* (Elsevier, 2012).
48. J. E. Tierney, M. P. Tingley, *Geochim. Cosmochim. Acta* **127**, 83–106 (2014).
49. J. Erez, B. Luz, *Geochim. Cosmochim. Acta* **47**, 1025–1031 (1983).

ACKNOWLEDGMENTS

We thank S. Oleynik, A. Weigand, B. Hinnenberg, and F. Rubach for laboratory support and expertise, and P. Mateo for advice on foraminifera picking. This research used samples and/or data provided by the Ocean Drilling Program (ODP) and the International Ocean Discovery Program (IODP). The manuscript was improved by comments from three anonymous reviewers. **Funding:** This work was supported by U.S. NSF grants OCE-1060947, 0960802, and 1136345 (D.M.S.) and by the Max Planck Society (G.H.H.); E.R.K. received support from the Tuttle Fund of the Department of Geosciences, Princeton University; D.A.S. was supported by the NOAA Climate and Global Change Postdoctoral Fellowship. **Author contributions:** D.A.S., D.M.S., and J.A.H. conceptualized the study; E.R.K. and D.A.S. carried out the nitrogen isotope measurements; A.A. and A.M.-G. carried out the TEX_{86} measurements; X.T.W. and H.R. provided methodology and training; E.R.K., D.A.S., J.A.H., and D.M.S. performed data analysis; E.R.K. and D.M.S. prepared the manuscript with input from all authors. **Competing interests:** The authors have no competing interests to declare. **Data and materials availability:** All data are available in the manuscript or the supplementary materials.

SUPPLEMENTARY MATERIALS

science.sciencemag.org/content/364/6438/386/suppl/DC1
Materials and Methods
Supplementary Text
Figs. S1 to S10
Tables S1 to S4
References (*50*–*85*)
Data S1 and S2

6 August 2018; accepted 26 March 2019
10.1126/science.aau5784

Nitrogen isotope evidence for expanded ocean suboxia in the early Cenozoic

Emma R. Kast, Daniel A. Stolper, Alexandra Auderset, John A. Higgins, Haojia Ren, Xingchen T. Wang, Alfredo Martínez-García, Gerald H. Haug, and Daniel M. Sigman

Science **364** (6438), . DOI: 10.1126/science.aau5784

Circulation more than temperature

Changes in continental configuration and sea level affected the ocean's oxygen levels and the rate of denitrification between 70 and 30 million years ago. That finding by Kast *et al.* shows a fundamental difference from the modern ocean, in which the extent of suboxia is controlled primarily by global temperature. Changes in the nitrogen isotopic composition of marine organic matter correlate with the collision of India and Asia and the circulation changes that occurred as a result. Later, isotopic composition changed further in response to a fall in sea level as global cooling caused ice sheets to grow.

Science, this issue p. 386

Science (ISSN 1095-9203) is published by the American Association for the Advancement of Science. 1200 New York Avenue NW, Washington, DC 20005. The title *Science* is a registered trademark of AAAS.